Lab on a Chip

Supplementary Information

Microfabricated acoustofluidic membrane acoustic waveguide actuator for highly localized in-droplet dynamic particle manipulation

Philippe Vachon*[ab], Srinivas Merugu[a], Jaibir Sharma[a], Amit Lal[ac], Eldwin J. Ng[a], Yul Koh[a], Joshua E.-Y. Lee[a], Chengkuo Lee[b]

* Email: philippe.vachon@u.nus.edu

[a.] *Institute of Microelectronics, A*STAR, Singapore.*
[b.] *Department of Electrical and Computer Engineering, National University of Singapore, Singapore.*
[c.] *SonicMEMS Laboratory, School of Electrical and Computer Engineering, Cornell University, Ithaca, USA.*

This file includes:

Supplementary Text
- Details of FEA numerical models
- Surface crater and bubble defects on the piezoelectric layer
- Particle tracking using Python and the module Trackpy v.0.5

Table S1
Figs. S1, S2, S3 and S4
Legends for movies S1 to S6
References (1-4)

Other Electronic Supplementary Materials for this manuscript include the following:

Movies S1 to S6
Data and Python code for Trackpy velocity extraction.

Details of FEA numerical models

Following COMSOL's Solid Mechanics definition of the time domain wave fields in the solid domain, see Structural Mechanics Module User's Guide [1], the equation of motion is given by

$$\rho_m \frac{\partial^2 \boldsymbol{u_{solid}}}{\partial t^2} = \nabla \cdot (FS)^{\mathrm{T}} + \boldsymbol{F_v} \quad \text{(S1)}$$

where ρ_m is the material density, $\boldsymbol{u_{solid}}$ is the displacement in the solid, *F* is the deformation gradient tensor, *S* is the second Piola-Kirchhoff stress tensor and $\boldsymbol{F_v}$ is the volume force vector.

The model comprises 3 material layers: the doped Si membrane, the AlScN piezoelectric thin film, and the Mo electrodes, which all have their own Linear Elastic Material or Piezoelectric Material node. Mo electrodes are modeled based on an isotropic solid, while the doped Si and AlScN are modeled on an anisotropic solid. The coordinate system used for the Si has been rotated by α = pi/4 to account for the Si (100) orientation. The Si segments at the end of the models were also assigned a progressive Rayleigh damping with α_{dM} = 0 and β_{dK} = -2.5E-9(1-exp(4.5(abs(x)-(0.0004))/(0.0012))), abs(x) ∈ [0.0004,0.0012] (for the right segment, different coordinates are used for the left segment), giving

$$\rho_m \frac{\partial^2 \boldsymbol{u_{solid}}}{\partial t^2} = \nabla \cdot \left((FS)^T + \beta_{dK} \frac{\partial (FS)^T}{\partial t} \right) + \boldsymbol{F_v} \quad \text{(S2)}$$

The AlScN is modeled with a Piezoelectric Material label settings in the Solid Mechanics module, with its constitutive relation in the form of the stress-charge formulation. All materials forming the waveguide are also bounded by two boundary conditions, the Fixed Constraint node boundary condition on the back side to simulate the bulk silicon clamping the membrane and the Symmetry node reduce the size of the model and form a cross-section in the middle of the membrane in the XZ plane, see supplementary Fig. S2.

In Electrostatics physics, a Charge Conservation, Piezoelectric node is added for the AlScN layer, which contributes to the governing equations by affecting the electric displacement field **D** as

$$\nabla \cdot \mathbf{D} = \rho_v \quad \text{(S3)}$$

where ρ_v is the volume charge density and

$$\mathbf{D} = \epsilon_0 det(F)\left(F^{\mathrm{T}}F\right)^{-1}(-\nabla \mathrm{V}) + \epsilon_0(\epsilon_{rS} - 1)(-\nabla \mathrm{V}) \quad \text{(S4)}$$

where ϵ_0 is the vacuum permittivity, *F* is the deformation gradient tensor, *V* is the electric potential and ϵ_{rS} is the relative permittivity.

The interface between the AlScN piezoelectric layer and the Si is set to ground via another node.

Two more Electric Potential nodes are added as boundaries under the positive and negative Mo electrodes to modulate the actuation voltage with a sine function.

The water loading the membrane is modeled using Pressure Acoustics, Transient physics.

The governing equation in the domain for a linear elastic fluid is the scalar wave equation,

$$\frac{1}{\rho_w c^2}\frac{\partial^2 p_t}{\partial t^2} + \nabla \cdot \left(\frac{-1}{\rho_w} (\nabla \mathrm{p_t} - \mathbf{q}_{\mathrm{d}}) \right) = \mathrm{Q_m} \quad \text{(S5)}$$

where ρ_w is the density of the water, p_t is the total pressure in the liquid, $\mathbf{q}_{\mathrm{d}}$ is the dipole domain source, and $\mathrm{Q_m}$ is the monopole domain source, the latter two being 0 in the bulk of the liquid. The Acoustic-Structure Boundary multiphysics module contributes to the right side of the equation on the boundary between the water domain and the solid membrane domain by matching the normal component of the pressure gradient to the normal acceleration of the membrane boundary, $\boldsymbol{n} \cdot \frac{\nabla p_t}{\rho_c} = \boldsymbol{n} \cdot \boldsymbol{u}_{tt}$. A symmetry node is also added to the XZ plane, while the other outer boundaries have their total pressure set to 0 via a Sound Soft Boundary node.

Surface crater and bubble defects on the piezoelectric layer

In some of the figures and movies, it can be seen that some devices observed under the optical microscope present top-side craters and bubble-like spots and defects. These features appeared on the AlScN layer during the etching step of the molybdenum electrodes forming the IDTs. During this step, some large areas of Si were left exposed, and as the Mo etch recipe used has a poor selectivity to Si, it may have caused the defect to appear. However, the affected devices bearing these defects have typically shown no change in their performance and acoustofluidic capabilities.

Particle tracking using Python and the module Trackpy v.0.5

To extract the particle velocity as a function of the actuation voltage amplitude, movies of the moving particles at different voltages were obtained and processed as a sequence of PNG pictures frame by frame. The picture sequences were then processed in Python using the module Trackpy [2]. By providing the image sequences, the frame rate and the real width of a pixel (µm/pixel), and tuning the parameters in Trackpy, it is possible to identify the particles and calculate their frame-by-frame displacement, see Fig. S4

The motion of the particle measured is the motion induced by the traveling guided flexural waves in their direction of propagation. However, the videos recorded often show particles coming from outside the membrane and slowly drifting onto the membrane during the alignment portion of the particle motion. This type of drag motion is not desired and will affect the velocity measured by the module. The parameters were tuned to ignore it as much as possible, but artifacts persist, especially at low voltages.
The desired velocity measured is the velocity of the aligned particles on the membrane. The velocity curve as a function of the actuation voltage amplitude is shown in Fig. 5 of the main paper. The error bars on the measurement points represent the standard deviation of the mean for the velocity of all the particles for each voltage amplitude.

The video frames and the Python code for the velocity extraction are available as ESI outside this document.

Table S1. Material properties used for numerical simulations.

Mo				
Density	ρ_m	10200	kg/m³	
Young's modulus	E	312	GPa	
Poisson's ratio	ν	0.31		
AlScN				
Density	ρ_m	3270	kg/m³	Interpolated from [3]
Elasticity matrix	C_E	$\begin{bmatrix} 351 & 143 & 109 & 0 & 0 & 0 \\ 143 & 351 & 109 & 0 & 0 & 0 \\ 109 & 109 & 300 & 0 & 0 & 0 \\ 0 & 0 & 0 & 111 & 0 & 0 \\ 0 & 0 & 0 & 0 & 111 & 0 \\ 0 & 0 & 0 & 0 & 0 & 104 \end{bmatrix}$	GPa	Interpolated from [3], [4]
Coupling matrix	e_{ES}	$\begin{bmatrix} 0 & 0 & -0.54 & 0 & -0.26 & 0 \\ 0 & 0 & -0.54 & -0.26 & 0 & 0 \\ -0.54 & -0.54 & 1.92 & 0 & 0 & 0 \\ 0 & -0.26 & 0 & 0 & 0 & 0 \\ -0.26 & 0 & 0 & 0 & 0 & 0 \\ 0 & 0 & 0 & 0 & 0 & 0 \end{bmatrix}$	C/m²	Interpolated from [3]
Relative permittivity	ε_r	12.3		
Phosphorus-doped Si				
Density	ρ_m	2330	kg/m³	
Elasticity matrix	D	$\begin{bmatrix} 146 & 60 & 60 & 0 & 0 & 0 \\ 60 & 146 & 60 & 0 & 0 & 0 \\ 60 & 60 & 146 & 0 & 0 & 0 \\ 0 & 0 & 0 & 69 & 0 & 0 \\ 0 & 0 & 0 & 0 & 69 & 0 \\ 0 & 0 & 0 & 0 & 0 & 69 \end{bmatrix}$	GPa	
Water				
Density	ρ_w	998.2	kg/m³	
Speed of sound	c	1481	m/s	

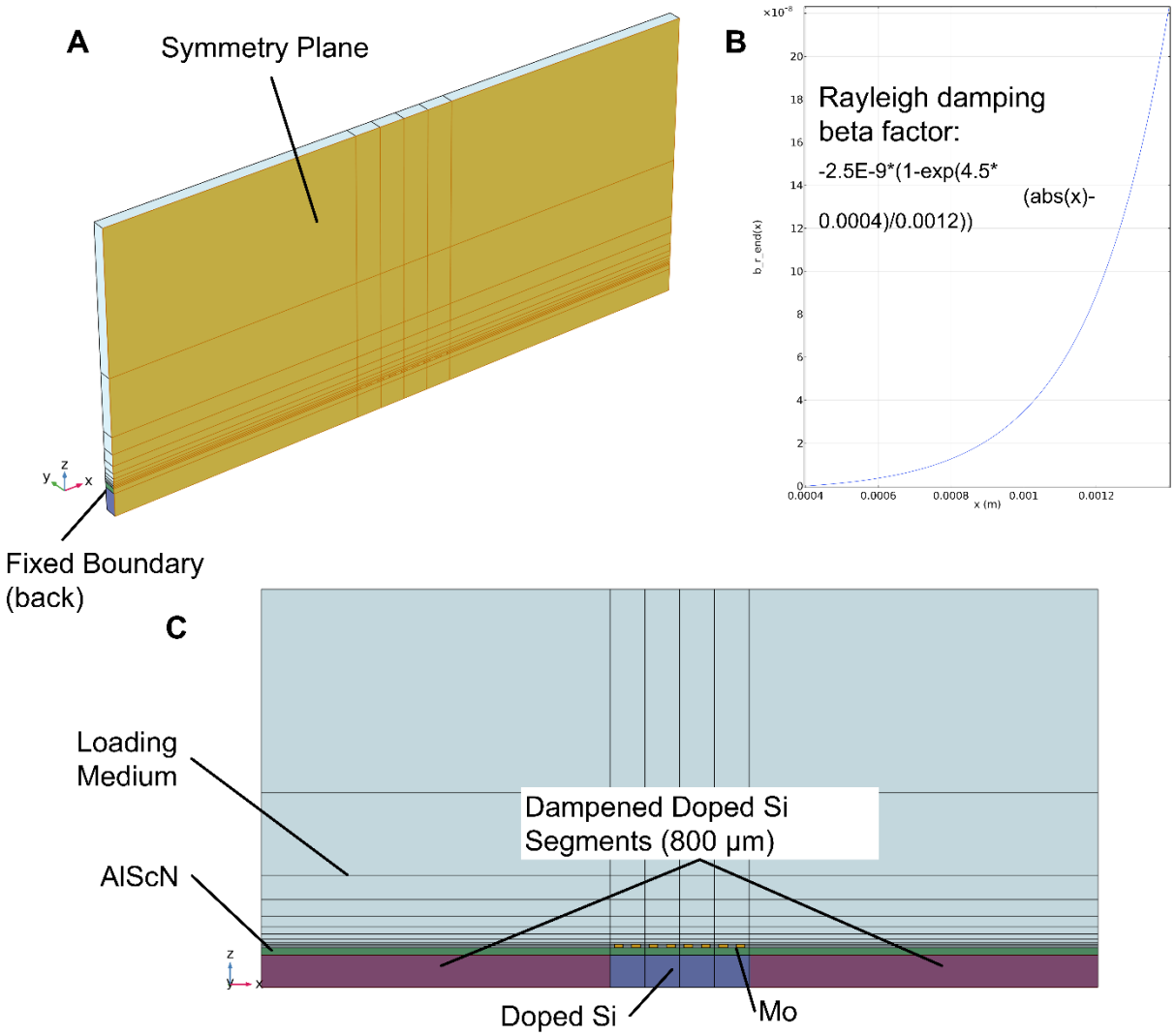

Fig. S1 **Main components of the 3D acousto-mechanical FEA model.** (**A**) Angled view of the 3D model with the symmetry plane in yellow, cutting the membrane in half, and the anchored boundary at the back. (**B**) Plot of the gradually increasing β_{dK} Rayleigh damping used to attenuate the vibrations on the end segments (specifically the right segment starting at x = 400 µm). (**C**) XZ plane view of the model, with colored parts. Loading medium (water) in light blue, doped Si in blue and burgundy, AlScN in green, and Mo in yellow. The total length of the membrane is 2000 µm.

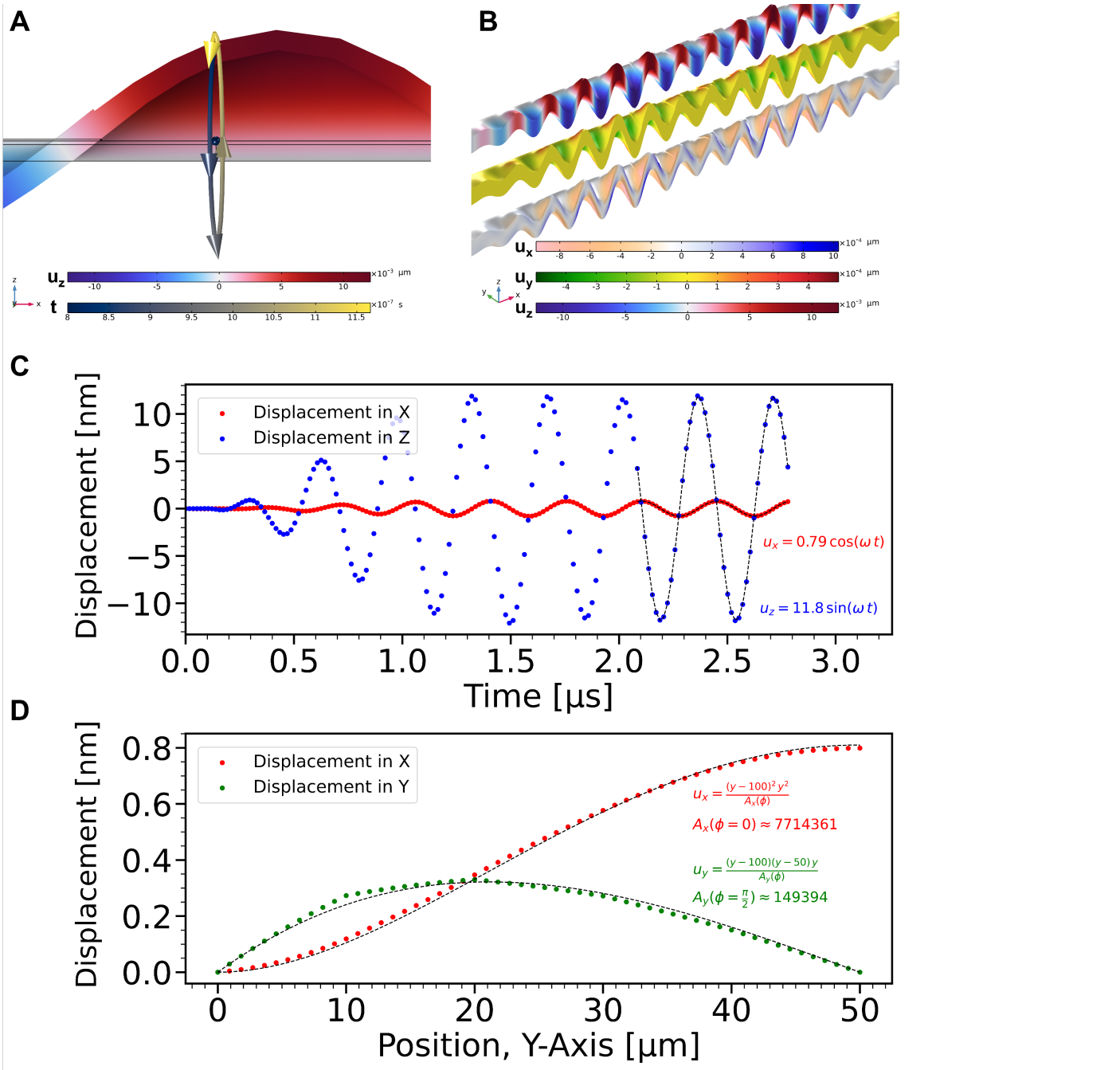

Fig. S2 **Particle motion representation and displacement fields in the solid membrane waveguide from the FEA model.** (**A**) Particle motion representation of a *material particle* at the top and in the center (y=50 µm) of the membrane waveguide, directly in contact with the loading water medium. The black dot represents the particle at rest. The elliptical shape with the arrows shows the particle motion during a full period of actuation. (**B**) Displacement vector fields $\boldsymbol{u}_x$, $\boldsymbol{u}_y$ and $\boldsymbol{u}_z$ in the membrane waveguide under actuation. (**C**) Time domain simulation of the displacement $\boldsymbol{u}_x$ and $\boldsymbol{u}_z$ of the material point in (A) with sine fit. (**D**) Cross-section of half the waveguide in the Y-direction showing the maximum displacement curve for $\boldsymbol{u}_x$ and $\boldsymbol{u}_y$ as a function of the y coordinate. The membrane clamped edge is at 0 and the center of the membrane is at 50 µm.

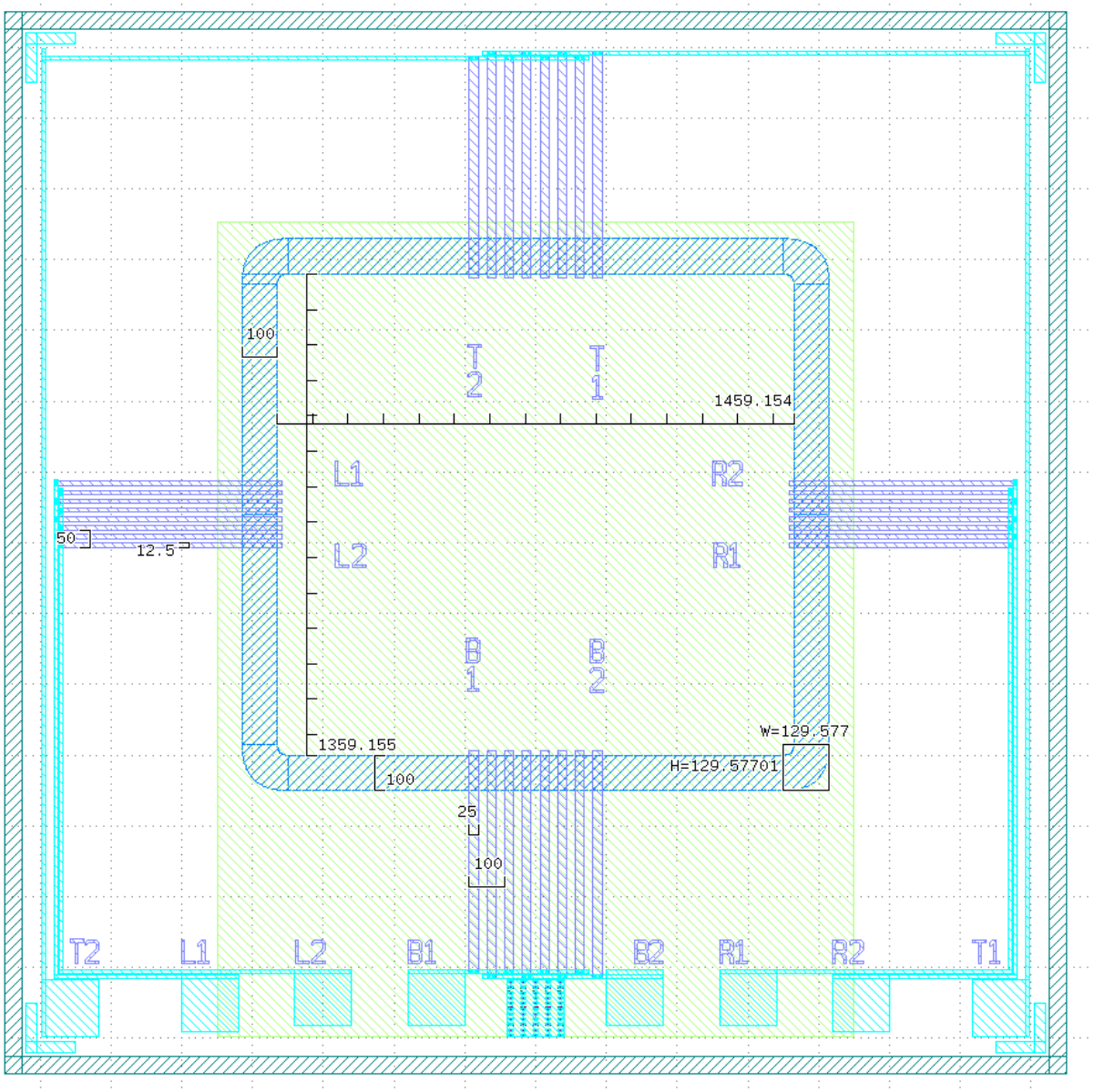

Fig. S3 **Fabrication layout of the MAWA device**. Layout of the different fabrication layers of the MAWA device with dimension (µm). The membrane is drawn in blue and annotated with the relevant dimensions. The Mo layer is purple, annotated with the IDTs dimensions. The Al layer is cyan. The doped area is light green.

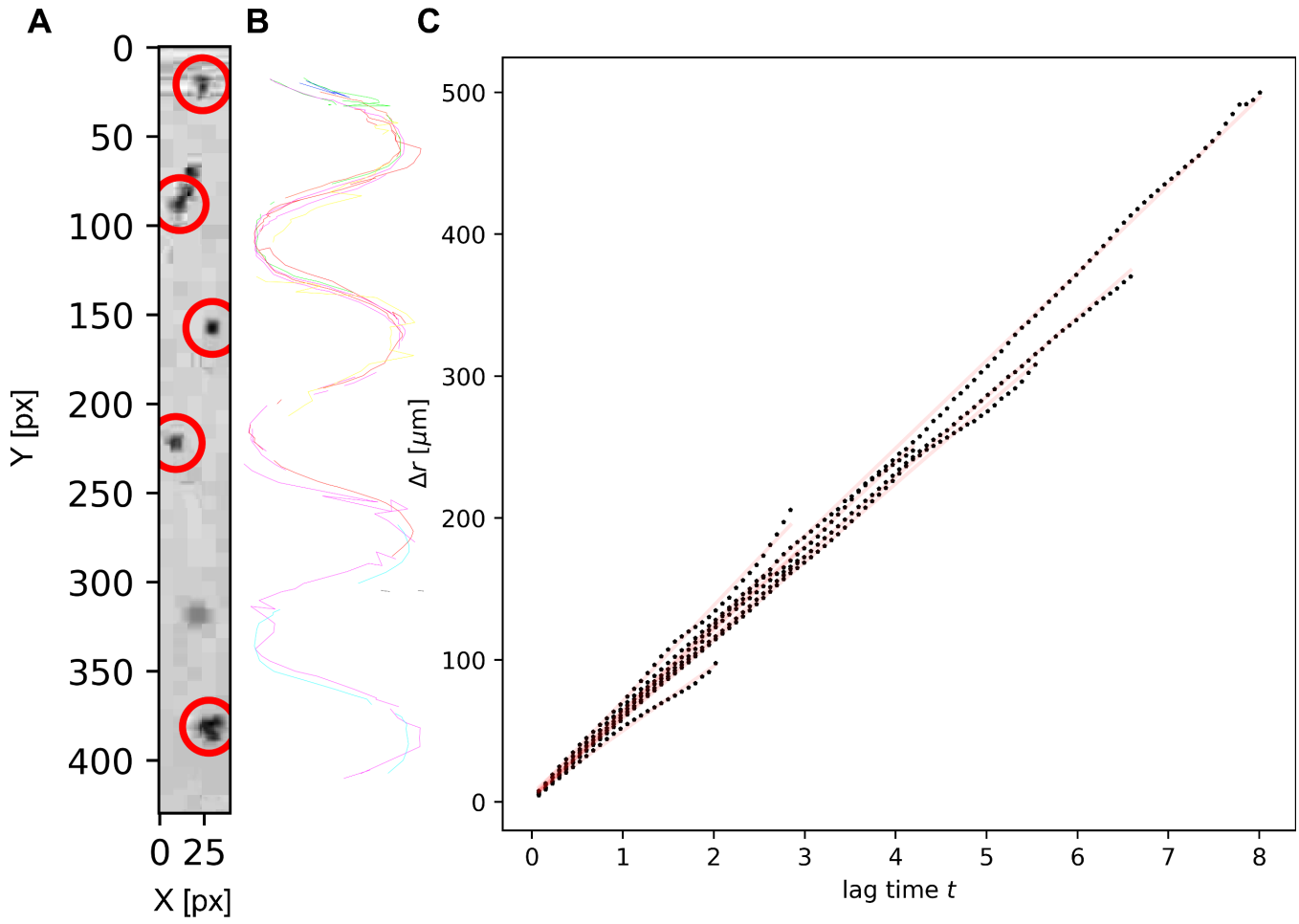

Fig. S4 **Particle detection and velocity extraction in Trackpy** (**A**) Software-based particle detection identifying 10 µm particles from a sequence of pictures made from the frames of videos recorded during experiments. (**B**) Traced transient trajectories of the filtered particles for all the processed frames. (**C**) Plotted frame-by-frame displacements of the particles as a function of time. The slope of each curve is extracted with a linear curve fit to give the velocity of a particle.

Legends for movies S1 to S6

Movie S1. Time domain simulation of GFWs on a linear membrane. Flexural waves are excited by 4 pairs of finger electrodes on the membrane. There is a β_{dK} Rayleigh damping on the end segments of the membrane. Actuation frequency is 2.85 MHz with 10 $V_{pk\text{-}pk}$. The top of the membrane is loaded with water. The top animation shows the top view of the half-depth membrane in the XY plane. The bottom animation shows the side view like a cross-section in the XZ plane.

Movie S2. Time domain simulation of GFWs on a corner membrane. Flexural waves are excited by 4 pairs of finger electrodes on the membrane. There is a β_{dK} Rayleigh damping on the end segments of the membrane. Actuation frequency is 2.85 MHz with 10 $V_{pk\text{-}pk}$. The top of the membrane is loaded with water. The waves can be seen propagating from the IDT and around the corner on the next segment.

Movie S3. Time domain LDV measurement of a burst of GFWs traveling on the membrane from the MAWA device. Burst of flexural waves excited by 4 pairs of finger electrodes composing the bottom IDT traveling in both directions on the membrane (highlighted in blue). Actuation frequency is 2.5 MHz with 10 $V_{pk\text{-}pk}$. The device is completely submerged in water. The video is slowed down, and its original duration is about 11 µs. Scale bar is 500 µm.

Movie S4. Time domain LDV measurement of GFWs traveling on the membrane from the MAWA device. Continuous sine actuation at the bottom IDT generating traveling GFWs in both directions on the membrane. Actuation frequency is 3.2234 MHz with 10 $V_{pk\text{-}pk}$. The device is completely submerged in water. The video is slowed down, and its original duration is about 1.55 µs. Scale bar is 500 µm.

Movie S5. Time domain LDV measurement of traveling GFWs forming standing and rotating waves on the membrane. Continuous sine actuation at the bottom and top IDTs generating standing waves on the right segment and rotating waves on the left segment. Actuation frequency is 3.16 MHz with 10 $V_{pk\text{-}pk}$. The device is completely submerged in water. The video is slowed down, and its original duration is about 0.95 µs. Scale bar is 500 µm.

Movie S6. Acoustofluidic experiment from Fig. 7. Dynamic continuous control of particles via GFWs. The device membrane is immersed in water from a droplet containing 5 µm polystyrene particles. The time stamps in Fig. 7 refer to the time in seconds of this movie. All parts are replayed in real-time. (1.) The first part of the movie features particles moving upward under the actuation of the bottom IDT 1 at 2.85 MHz. Half of the top IDT electrodes were also active during this time, in beating mode, but their effect did not affect the intended demonstration, and the explanation for their contribution is beyond the scope of this experiment. Both IDTs are stopped at the end of this part. (2.) The movie's second part features particles moving downward under the actuation of the top IDT 1, also at 2.85 MHz. The actuation is stopped once the particles have reached the bottom segment of the membrane. (3.) The third part of the movie features particles trapped in rotating rings under the actuation of the top and bottom IDTs 1 at 3.05 MHz. Immobile particles first migrate toward the left segment once the actuation is on, then progressively form visible rings as more particles migrate and get trapped on the membrane. (4.) In the fourth part of the movie, both IDTs 1 are active, and the frequency is changed to 3.15 MHz. The rotating particles migrate to form periodically spaced fixed clusters on the membrane. (5.) In the fifth and last part of the movie, both IDTs 1 are stopped, and the left IDT 2 is activated at 9.8 MHz. The particles are split into two groups that travel toward the top and the bottom under the actuation.

References

[1] "Structural Mechanics Module User's Guide," *COMSOL Multiphysics® v. 6.1*. COMSOL AB, Stockholm, Sweden, 2022. [Online]. Available: https://doc.comsol.com/6.1/doc/com.comsol.help.sme/StructuralMechanicsModuleUsersGuide.pdf

[2] D. B. Allan, T. Caswell, N. C. Keim, C. M. van der Wel, and R. W. Verweij, "soft-matter/trackpy: Trackpy v0.5.0," Apr. 2021, doi: 10.5281/ZENODO.4682814.

[3] N. Kurz *et al.*, "Experimental determination of the electro-acoustic properties of thin film AlScN using surface acoustic wave resonators," *J. Appl. Phys.*, vol. 126, no. 7, p. 075106, Aug. 2019, doi: 10.1063/1.5094611.

[4] M. A. Caro *et al.*, "Piezoelectric coefficients and spontaneous polarization of ScAlN," *J. Phys. Condens. Matter*, vol. 27, no. 24, p. 245901, Jun. 2015, doi: 10.1088/0953-8984/27/24/245901.